THE JOURNAL OF BIOLOGICAL CHEMISTRY
Vol. 279, No. 27, Issue of July 2, pp. 28202–28208, 2004

Printed in U.S.A.

Structures and Analysis of Highly Homologous Psychrophilic, Mesophilic, and Thermophilic Adenylate Kinases*

Received for publication, February 20, 2004, and in revised form, April 19, 2004
Published, JBC Papers in Press, April 20, 2004, DOI 10.1074/jbc.M401865200

Euiyoung Bae and George N. Phillips, Jr.‡

From the Department of Biochemistry, University of Wisconsin, Madison, Wisconsin 53706

The crystal structures of adenylate kinases from the psychrophile *Bacillus globisporus* and the mesophile *Bacillus subtilis* have been solved and compared with that from the thermophile *Bacillus stearothermophilus*. This is the first example we know of where a trio of protein structures has been solved that have the same number of amino acids and a high level of identity (66–74%) and yet come from organisms with different operating temperatures. The enzymes were characterized for their own thermal denaturation and inactivation, and they exhibited the same temperature preferences as their source organisms. The structures of the three highly homologous, dynamic proteins with different temperature-activity profiles provide an opportunity to explore a molecular mechanism of cold and heat adaptation. Their analysis suggests that the maintenance of the balance between stability and flexibility is crucial for proteins to function at their environmental temperatures, and it is achieved by the modification of intramolecular interactions in the process of temperature adaptation.

There has recently been an increase in the discovery, isolation, and investigation of organisms inhabiting extreme environments (extremophiles) (1). Among these, organisms living at low and high temperatures (psychrophiles and thermophiles, respectively) have been of particular interest since proteins isolated from these organisms can function and remain stable at or near extreme temperatures (2, 3). These proteins have potential in industry directly or as models for engineering proteins from organisms living at moderate temperatures (mesophiles) because their unique properties such as activity at extreme temperatures and inactivity or instability at moderate temperatures are often desirable for industrial processes (4, 5). They have also drawn attention from academia because they provide a unique opportunity to study relationships between stability, dynamics, and function of proteins (6, 7). Therefore, research efforts have focused on comparative studies using proteins from temperature extremophiles and their mesophilic counterparts to illustrate a mechanism for temperature adaptation of proteins.

Because of the relative ease of crystallizing thermophilic proteins, many structural studies have been performed to identify the molecular basis of heat adaptation by comparing thermophilic proteins with their mesophilic homologs. Several unique structural features in thermophilic proteins have been observed (8). The modification of subtle intramolecular interactions such as hydrogen bonding (9), electrostatic interactions of ion pairs (10), and hydrophobic interactions (11) was proposed to be responsible for the increased thermal stability. On the other hand, the molecular mechanism of cold adaptation in psychrophilic proteins is still relatively unknown due to the limited number of available structures. In fact, only a handful of crystal structures have been solved for psychrophilic proteins presumably because their thermolability and flexibility cause difficulties in handling and crystallizing (12). However, a general feature of cold adaptation has begun to appear. Almost all the psychrophilic protein structures seem to contain fewer intramolecular interactions of the type involved in stabilization of thermophilic proteins at high temperatures (13–15). Each protein uses different specific structural strategies for cold adaptation (16). This phenomenon is understood in terms of maintaining appropriate flexibility to ensure physiological activity at different temperatures (17, 18). The hypothesis is that directed thermal motion is needed for catalysis, and thus, psychrophilic enzymes have to increase their flexibility at low temperatures by decreasing stability. According to this hypothesis, mesophilic enzymes essentially become too inflexible to perform a catalytic cycle at low temperatures, and the same phenomenon happens even at moderate temperatures for thermophilic enzymes.

Despite a growing abundance of comparative studies on temperature adaptation of proteins, most have been criticized because the proteins compared are often from distantly related organisms (19). These organisms probably experienced different evolutionary pressures that may or may not be related to temperature adaptation. Differences between protein structures may result from other sources than environmental temperatures. To minimize the phylogenetic noise, it is desirable to compare proteins from organisms that are closely related but inhabit different temperatures.

In this work we use adenylate kinases from the psychrophile *Bacillus globisporus* (AKglo)[1] (20), the mesophile *Bacillus sub-*

* This work was supported by a Vilas Associate Award (to G. N. P.) and the Wisconsin Alumni Research Foundation. Use of the Advanced Photon Source was supported by the United States Department of Energy, Basic Energy Sciences, Office of Science under Contract W-31-109-Eng-38. Use of the BioCARS beamline was supported by the National Institutes of Health, National Center for Research Resources under Grant number RR07707. Use of the Biophysics Instrumentation Facility was supported by the University of Wisconsin-Madison, National Science Foundation Grant BIR-9512577, and National Institutes of Health Grant S10 RR13790. The costs of publication of this article were defrayed in part by the payment of page charges. This article must therefore be hereby marked "*advertisement*" in accordance with 18 U.S.C. Section 1734 solely to indicate this fact.

The atomic coordinates and structure factors (codes 1S3G and 1P3J) have been deposited in the Protein Data Bank, Research Collaboratory for Structural Bioinformatics, Rutgers University, New Brunswick, NJ (http://www.rcsb.org/).

‡ To whom correspondence should be addressed: Dept. of Biochemistry, University of Wisconsin, 433 Babcock Dr., Madison, WI 53706. Tel.: 608-263-6142; Fax: 608-262-3453; E-mail: phillips@biochem.wisc.edu.

[1] The abbreviations used are: AKglo, adenylate kinase from *B. globisporus*; AKsub, adenylate kinase from *B. subtilis*; AKste, adenylate kinase from *B. stearothermophilus*; AK, adenylate kinase; Ap5A, P^1,P^5-di(adenosine 5′)-pentaphosphate; DSC, differential scanning calorimetry; T_m, thermal denaturation midpoint; CHES, 2-(cyclohexylamino)-ethanesulfonic acid.

tilis (AKsub) (21), and the thermophile *Bacillus stearothermophilus* (AKste) (22) to study cold and heat adaptation (23). They come from organisms in the same genus and exhibit a high level of similarity to ensure conservation of the structural features responsible for temperature adaptation. Adenylate kinase (AK), originally named myokinase because of its discovery in muscle, has been well studied over several decades (24). It undergoes substantial dynamic events during a catalytic cycle (25, 26). It has a LID domain that closes over the site of phosphoryl transfer and an AMP binding domain that closes on AMP when it is bound. Structures have been solved of various states of the enzyme from various species (11, 27–30) such that a firm basis for structural and dynamics studies has been established. By having a set of three highly dynamic targets with high sequence identity (about 70%) and differing temperature/activity and stability profiles we feel we have a special opportunity to explore the structure/dynamics/function relationships involved in the temperature adaptation of proteins.

EXPERIMENTAL PROCEDURES

Cloning, Expression, and Purification—AKglo and AKsub were commercially cloned by ATG Laboratories. To clone the unknown AKglo gene, 5′ and internal primers were designed based on other *Bacillus* AK sequences and the AKglo partial amino acid sequence provided by Dr. A.-M. Gilles and Dr. O. Bârzu. Amplification with these primers produced the 5′ end fragment. The sequence of the 3′ end of the gene was obtained using the inverse PCR strategy. The final sequence was confirmed by cloning and sequencing the full-length AKglo. The AKsub gene was cloned based on the known sequence. These genes were subcloned into *Escherichia coli* expression vectors, which were subsequently transformed into *E. coli* expression strain BL21[DE3].

The *E. coli* cells were grown at 37 °C until the optical density at 600 nm reached 0.7. Protein expression was then induced for 6 h by the addition of isopropyl-β-D-thiogalactopyranoside to 1 mM (final concentration). The cells were harvested by centrifugation, resuspended in 20 mM Tris-HCl (pH 7.8), 50 mM KCl, 10 mM $MgCl_2$ and lysed mechanically. The cell lysate was centrifuged, and the supernatant was collected for purification.

The proteins were purified at room temperature by affinity and gel filtration chromatography. After applying the crude extract to a column containing Bio-Rad Affi-Gel blue resin and washing with buffer (20 mM Tris-HCl (pH 7.8), 50 mM KCl, 10 mM $MgCl_2$), absorbed proteins were eluted by using a NaCl step gradient. The pooled fractions containing the enzymes were concentrated and applied to a Sephacryl S-200 HR gel filtration column from Amersham Biosciences. The fractions were collected by monitoring UV absorbance at 280 nm and were dialyzed against 10 mM Hepes (pH 7.0) and concentrated for crystallization. The proteins were judged to be pure by SDS-PAGE, and their concentrations were determined by UV absorbance at 280 nm. AKste was purchased from Sigma and used without further purification.

Differential Scanning Calorimetry—To study thermal stability of AKs and their complexes with inhibitor Ap5A, differential scanning calorimetry (DSC) was performed using a MicroCal MCS DSC instrument at a scanning rate of 1 °C/min. The samples were dialyzed against 50 mM Hepes (pH 7.4) and diluted with the buffer so that protein concentration in the sample would be 1 mg/ml. Buffer-buffer scans were also performed and subtracted from sample-buffer scans to minimize the background noise. Data were analyzed using MicroCal Origin provided by MicroCal.

Activity Assays—The enzyme activity of AKs was determined at various temperatures in the direction of ATP formation by an end-point method. AK (0.0001 mg/ml final concentration) was added to a 1-ml mixture containing 1 mM glucose, 0.4 mM $NADP^+$, 100 mM KCl, 2 mM $MgCl_2$, and 50 mM Hepes (pH 7.4). This assay solution was incubated at the desired temperature for 10 min, and the reaction was started by adding ADP (2.5 mM final concentration). The reaction was allowed to proceed at the same temperature for 3 min and then stopped by adding Ap5A (1 mM final concentration) and cooling on ice for 2 min. The amount of ATP produced by AK was determined using the ATP-dependent reduction of $NADP^+$ to NADPH. After adding 10 units of hexokinase and glucose-6-phosphate dehydrogenase, the reaction was allowed to complete at room temperature for 10 min, and then absorbance at 340 nm was measured. The experiments were repeated several times at each temperature.

Crystallization and Data Collection—Crystals of AKglo were grown by the small scale batch method (31) by mixing 4 μl of 20 mg/ml AKglo, 5 mM Ap5A with 6 μl of 2.5 M $(NH_4)_2SO_4$, 1% (w/v) polyethylene glycol 1000, 0.1% (w/v) NaN_3, 50 mM Hepes (pH 7.0). Crystals with hexagonal rod shape were grown to 0.5 mm long with a 0.04-mm edge of hexagon in 3 weeks at 20 °C. AKglo crystals were equilibrated for 30 s in 23% (v/v) glycerol, 2.1 M $(NH_4)_2SO_4$, 1% (w/v) polyethylene glycol 1000, 0.1% (w/v) NaN_3, 50 mM Hepes (pH 7.0) and then flash-frozen by transferring into cold liquid nitrogen. Diffraction data for AKglo were collected on a MARCCD-165 detector at the BioCARS 14-ID-B beamline of the Advanced Photon Source.

Crystals of AKsub were grown by the hanging-drop method. The drops were made by mixing 6 μl of 18 mg/ml AKsub and 3.5 mM Ap5A with 6 μl of the crystallization solution containing 35% (w/v) polyethylene glycol 1500, 50 mM $CaCl_2$, 50 mM CHES (pH 9.0). Crystals with rectangular block shape grew to dimensions of $0.1 \times 0.05 \times 0.05$ mm in 5 days at 20 °C. AKsub crystals were flash-frozen in a cold liquid nitrogen stream directly from the drops without any cryoprotectant. Diffraction data for AKsub were collected on an ADSC Q-4 detector at the BioCARS 14-BM-D beamline of the Advanced Photon Source.

Data Processing, Molecular Replacement, and Refinement—The data for AKglo and AKsub were processed with the HKL program package (32). A molecular replacement solution for AKsub was found using SOMoRe (33) with the molecular model of AKste (PDB entry 1ZIN). After refinement steps, the new AKsub model was used to solve the AKglo structure by molecular replacement.

Both AK structures were refined with CNS (34) and XtalView (35). The refinement with cycles of energy minimization, temperature factor fitting, manual rebuilding, and solvent addition continued until no improvement was observed in R and R_{free}. No restraints were used between metal ions and their coordinated atoms in the refinement.

Structure Analysis—Structure quality was evaluated using PROCHECK (36). Structure superposition was performed with Sequoia (37). Two oppositely charged residues were identified as an ion pair if their closest oppositely charged atoms were within 4 Å. The carboxylic oxygen atoms of Asp, Glu, and the C-terminal residue were considered as negatively charged atoms, and the amino nitrogen atoms of Arg, Lys, His, and the N-terminal residue were considered as positively charged atoms. Hydrogen bonds were defined by using HB2 options in WHAT IF (38). In the HB2 options the total hydrogen bonding energy is optimized to find the best positions for all hydrogen atoms simultaneously, and hydrogen bonds are determined from the donor/acceptor types, the H-acceptor distance, the donor-H-acceptor angle, and the position of the hydrogen with respect to the acceptor. Polar and apolar-exposed and buried surface areas were calculated with WHAT IF using a probe radius of 1.4 Å. Nitrogen and oxygen atoms were considered polar, and carbon and sulfur atoms were considered apolar. All properties were analyzed for residues 1–212 and averaged over multiple conformations. Among three structures of AKste, the Mg^{2+}Ap5A-bound form (PDB entry 1ZIO) was used for analysis. All figures with molecular structures have been generated using RIBBONS (39).

RESULTS

Sequence Comparison—Newly sequenced AKglo has been aligned with AKsub and AKste in Fig. 1. They have the same number of amino acids and could be aligned without any gap. As expected, they share high amino acid sequence identity; 67% for AKglo and AKsub, 74% for AKsub and AKste, and 66% for AKste and AKglo. The N-terminal region is well conserved, including the completely conserved P-loop region (residues 7–15), whereas the C-terminal region is the most variable. As in other AKs from Gram-positive bacteria, AKglo contains the sequence Cys-X_2-Cys-X_{16}-Cys-X_2-Cys/Asp, which is involved in zinc coordination (20). AKglo has Asp-153 at the last position of the motif identical to AKsub.

Thermal Stability and Temperature Optimum—Thermal denaturation midpoints (T_m) of AKglo, AKsub, and their Ap5A complexes were determined by DSC experiments (Table I). The scans were performed from 5 to 85 °C. The resulting data clearly showed a single peak for each scan and, therefore, can be well approximated by a two-state transition model. The T_m of AKsub (47.6 °C) is similar to the previously reported value (50.7 °C) considering that different conditions were used for DSC in the previous study (21). Ap5A complexes of AKglo and AKsub have higher T_m values than the

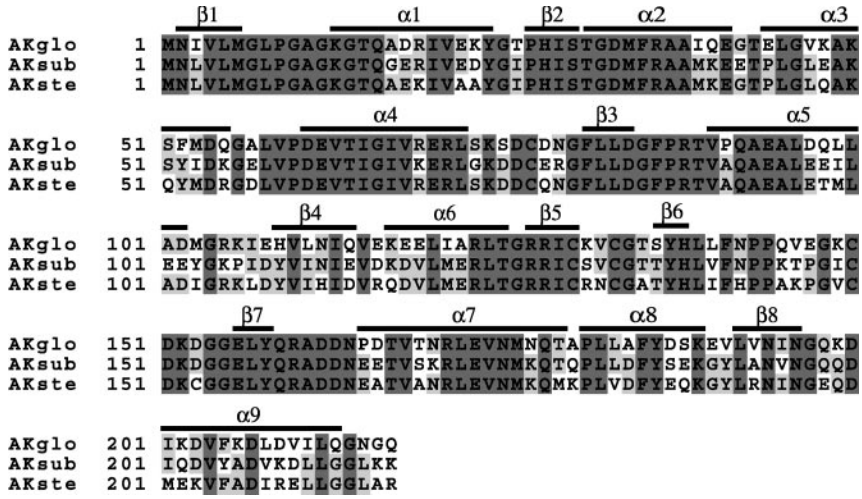

FIG. 1. **Sequence alignment of *Bacillus* AKs.** The sequences can be aligned without any gap by the program ClustalW (50). They share high amino acid sequence identity; 67% for AKglo and AKsub, 74% for AKsub and AKste, and 66% for AKste and AKglo. The secondary structures of AKste are indicated.

TABLE I
Thermal denaturation midpoint (Tm) of Bacillus AKs

Enzyme	T_m	T_m of Ap5A complex
	°C	°C
AKglo	43.3	60.4
AKsub	47.6	66.0
AKste[a]	>55.0	>70.0

[a] Temperature scans for AKste and AKste·Ap5A complex were ended at 55 and 70 °C, respectively, and no signal for transition was observed.

free AKs, but the T_m difference between AKglo and AKsub is maintained between AKglo·Ap5A and AKsub·Ap5A complexes. No attempt to measure T_m values for AKste and the AKste·Ap5A complex was made because in preliminary temperature scans they started to precipitate at about 60 and 80 °C, respectively. This does not mean that they are not stable below the temperatures where precipitation takes place. To show stability of AKste and the AKste·Ap5A complex before precipitation, temperature scans for the DSC experiments were performed to 55 and 70 °C, respectively, and no signal for transition was observed. Considering this observation and the previously reported T_m for AKste of 74.5 °C (22), it would be reasonable to assume that T_m values of AKste and its Ap5A complex are at least higher than 55 and 70 °C, respectively, indicating that AKste is the most stable among the three AKs, and the AKste·Ap5A complex is more stable than the AKglo·Ap5A and AKsub·Ap5A complexes.

AKglo, AKsub, and AKste have disparate optimal temperatures for their AK activity, which reflect temperature optima of their psychrophilic, mesophilic, and thermophilic source organisms (Fig. 2). The three temperature profiles have similar shapes and could be overlapped by shifting toward high or low temperatures, indicating temperature adaptation. Psychrophilic AKglo showed the lowest temperature optimum as well as higher relative activity at lower temperatures than AKsub and AKste. Thermophilic AKste displayed its maximum activity at high temperatures, where AKglo and AKsub are completely inactive. In the assays, altering the preheating time before starting the reactions caused changes in the temperature optimum (data not shown). Longer incubation of AKs resulted in shifting of the temperature profiles toward low temperatures, indicating that at temperatures even below their denaturation temperatures (T_m values), long exposure of AKs to heat caused continuous gradual denaturation. However, the ordering in temperature optima of AKglo, AKsub, and AKste was always observed with different preheating times. Therefore, the data presented here, which were obtained with 10-min

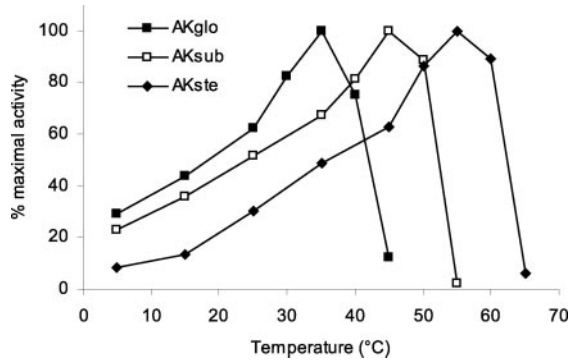

FIG. 2. **Temperature profiles for the activity of *Bacillus* AKs.** They have disparate optimal temperatures for AK activity reflecting temperature optima of their source organisms. Curves represent the average of three independent experiments, and the standard error of each average is less than 5%.

preheating times should be interpreted to illustrate different relative temperature-activity profiles of the three AKs rather than used to give a specific optimal temperature for each AK.

Structure Overview—The crystal structures of AKglo and AKsub were solved to resolutions of 2.25 and 1.90 Å, respectively. A summary of data collection and refinement statistics is presented in Table II. Both AKs were crystallized with a bound inhibitor, Ap5A, in their active sites. Residues 213–217 of AKsub are missing from the model due to disorder of the C terminus, whereas the AKglo model contains all 217 residues. Ramachandran plots indicate that for AKglo and AKsub, 90.8 and 92.7% of non-Gly and non-Pro residues fall in the most favored regions, and 9.2 and 7.3% fall in the allowed regions, respectively.

The chain folds of AKglo and AKsub are essentially identical to those of other AKs. Both structures are composed of a central β-sheet and surrounding α-helices and possess the three characteristic AK domains CORE (residues 1–30, 60–127, and 160–217), AMP binding (residues 31–59), and LID (residues 128–159). The structures of the three *Bacillus* AKs are very similar except for the position of the LID domain (Fig. 3). AKglo and AKsub have their LID domains fully closed, but AKste has a partially opened LID domain, which was previously attributed to packing contacts within the AKste crystal (29). Alignments of the three LID domains confirm that the LID domain of AKste has moved as a rigid body (Table III).

AKglo and AKsub were known to have a Zn^{2+} atom in their LID domains (20). In both AKglo and AKsub, the bound Zn^{2+} atom is very obvious in the LID domain and is coordinated to Cys-130, Cys-133, Cys-150, and Asp-153 (Fig. 4), whereas in

TABLE II
Crystallographic data statistics

	AKglo[a]	AKsub[a]	AKste[b]
Space group	$P3_121$	$P2_1$	$P2_1$
Cell constants	65.3 Å × 65.3 Å × 94.4 Å	32.8 Å × 73.2 Å × 38.1 Å, β = 101.6°	41.2 Å × 62.3 Å × 42.1 Å, β = 117.1°
Resolution (Å)	2.25 (2.33–2.25)	1.90 (1.97–1.90)	1.96
Unique reflections	11,384 (1112)	13,641 (1084)	12,454
Completeness (%)	99.2 (99.4)	96.8 (76.3)	93.1
R_{merge} (%)	5.7 (59.3)	5.0 (16.6)	10.6
R (%)	22.3	19.7	16.1
R_{free} (%)	28.8	24.6	22.8
r.m.s.d.[c] from ideality			
Bonds (Å)	0.017	0.021	0.012
Angles (°)	1.2	1.2	2.0
Average B-factors (Å^2)			
Main chain[d]	49.5	27.7	10.9
Side chain[d]	53.0	36.2	19.4
Solvent	49.8	37.5	28.0
Ap5A	37.7	21.3	8.7
Wilson plot B-factors (Å^2)	32.6	19.2	8.0

[a] Values in parentheses represent the highest resolution shell.
[b] Ref. 29.
[c] Root mean square deviation.
[d] Calculated for residues 1–212.

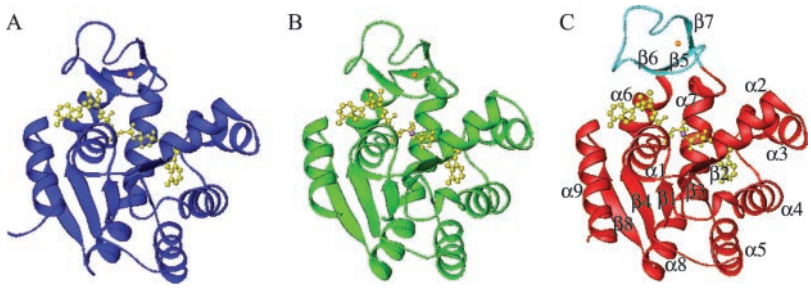

FIG. 3. **Structures of psychrophilic AKglo (*A*), mesophilic AKsub (*B*), and thermophilic AKste (*C*).** The structures are very similar except the position of the LID domain. The bound Zn^{2+} atoms are shown as *orange spheres* in the LID domain of each enzyme. The Ap5A molecules at their active sites are shown in *yellow*, and Mg^{2+} atoms in AKsub and AKste are represented as *purple spheres*. In *C*, the LID domain of AKste is shown in *cyan* to demonstrate the partially opened conformation, and the secondary structures are identified.

TABLE III
Root mean square deviation (r.m.s.d.) values for Cα atoms between Bacillus AKs

Domains aligned (residues)	Structures compared	r.m.s.d.	Residues not structurally equivalent[a]
		Å	
All (1–212)	AKglo-AKsub	0.73	None
	AKglo-AKste	1.65	132–135, 145–155
	AKsub-AKste	1.76	132–135, 145–155
LID (128–159)	AKglo-AKsub	0.40	None
	AKglo-AKste	0.43	None
	AKsub-AKste	0.40	None
CORE and AMP-binding (1–127, 160–212)	AKglo-AKsub	0.63	None
	AKglo-AKste	0.61	None
	AKsub-AKste	0.66	None

[a] Defined by the program Sequoia with the default distance cutoff (4.5 Å).

AKste the zinc ion is tetrahedrally coordinated to four Cys residues. They are the first protein structures to show zinc coordinated by three Cys and one Asp/Glu. The carboxylate of Asp-153 in both AKglo and AKsub shows bidentate coordination to the Zn^{2+} atom, and one of the connections between the Zn^{2+} and the carboxylic oxygens is longer than the other, as is usually found in bidentate arrangements within zinc binding sites in protein and small molecule structures (40).

Ap5A binding in both AKglo and AKsub exhibits the same general conformation as in AKste. The bound Ap5A occupies both ATP/ADP and AMP/ADP sites, and the side chains interacting with Ap5A are essentially the same in all three AKs. The AKglo structure does not have Mg^{2+} with the bound Ap5A, as is the case with other AK structures crystallized in ammonium sulfate solution (28, 29), but does not display alternative conformations of the δ phosphate seen in other structures having Ap5A without bound Mg^{2+}. The AKsub structure has Mg^{2+} with Ap5A and demonstrates hexagonal coordination with two phosphate oxygens in Ap5A and four water molecules as in the AKste structure.

Comparison of Structural Features—To reveal a molecular basis of low and high temperature adaptation, several structural features were compared between the three AK structures (Table IV). Ion pairs were identified using a distance cutoff of 4 Å. The thermophilic AKste has the most ion pairs among all three AKs, whereas the mesophilic AKsub has one less ion pair than the psychrophilic AKglo, which makes sense considering that ion pairs contribute to protein stability mostly at elevated temperatures (41). To make a more precise comparison of ion pairs rather than just counting the number of them with a

simple distance cutoff, a new concept called "critical ion pair" was introduced. Ion pairs were defined as critical if they bridge the distant regions of a polypeptide (more than 10 residues), and corresponding residues in the homologous counterpart do not form an ion pair either because at least one of the two residues is substituted or because the two residues are too far from each other (a distance cutoff of 6 Å). In the definition of critical ion pairs it is natural to rule out the conserved ion pairs, and it is also reasonable to stress ion pairs formed by residues from distant parts of a polypeptide because they are most likely not maintained in the unfolded state and, therefore, contribute to stability only in the folded state. The critical ion pairs are defined relatively and only for a pair of structures. The numbers of critical ion pairs are 4–0 for AKste-AKsub, 4–2 for AKste-AKglo, and 0–0 for AKsub-AKglo (Table V). One of the two critical ion pairs of AKglo relative to AKste, Lys-152—Asp-18, should be excluded from consideration since the corresponding ion pair in AKste may be formed if its LID domain is fully closed like AKglo. Consequently, AKste has three to four more critical ion pairs than AKglo and AKsub.

Even though the number of hydrogen bonds increases as thermostability increases in the trio of AKs, the differences are small, and whether these modest changes can cause a substantial effect on temperature adaptation is not known. Also, the degree to which hydrogen bonds contribute to protein stability has been controversial (42). Therefore, to correlate the number of hydrogen bonds with temperature adaptation, a large difference in the number might be required as in the case of *Thermus aquaticus* D-glyceraldehyde-3-phosphate dehydrogenase (9), in which the difference in the number of hydrogen bonds between the thermophilic protein and its counterpart is about 450. Considering the small differences in the number of hydrogen bonds between the *Bacillus* AKs, it is not clear whether they play an important role for heat or cold adaptation of the AKs.

Exposed and buried surface areas were calculated and analyzed for polar (N and O) and apolar (C and S) atoms. Apolar buried surface areas, which are usually used to estimate hydrophobic effect, are found to correlate with thermal stability. The thermophilic AKste has the most apolar buried surface area, and the psychrophilic AKglo has the least. The differences between AKste and AKsub and between AKsub and AKglo are 251 and 483 Å^2, respectively, which could be equivalent to 2.1–5.6 and 4.0–10.8 kcal/mol, respectively, if calculated as previously suggested (11). Interestingly, AKglo has the most apolar-exposed surface area, although it has the fewest apolar atoms.

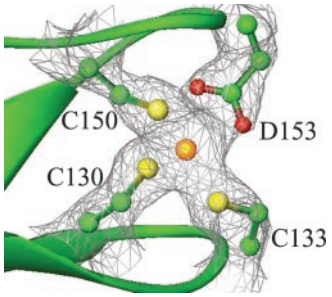

FIG. 4. **Zn^{2+} coordination in AKsub.** The zinc ion is ligated to three Cys and one Asp. The structure of this arrangement is revealed for the first time in this study. The zinc coordination is virtually identical in AKglo and AKsub structures. Electron density at the 1σ contour level is shown with the Zn^{2+} atom (shown in *orange*) and its four liganding residues.

TABLE IV
Comparison of structural features of Bacillus AKs

	AKglo[a]	AKsub[a]	AKste
Number of ion pairs	13	12	15
Number of hydrogen bonds	228.5	231.5	233
Number of apolar atoms[b]	1034	1048	1049
Buried surface area (Å^2)	15065	15548	15799
Exposed surface area (Å^2)	5638	5444	5408
Number of polar atoms[c]	604	607	605
Buried surface area (Å^2)	9750	9785	9797
Exposed surface area (Å^2)	4755	4581	4748

[a] Average values of multiple conformers.
[b] C and S.
[c] N and O.

DISCUSSION

The trio of AKs in this study provides a unique opportunity to study cold and heat adaptation of proteins from temperature extremophiles. Unlike other studies in which protein targets are evolutionary distant and sequence difference related to temperature adaptation may be masked by random or other sources of genetic drift, the *Bacillus* AKs have exactly the same number of amino acids and share a high level of sequence identity. This is the first example we know of where structures have been solved for three orthologous proteins that come from psychrophilic, mesophilic, and thermophilic organisms in the same genus. The dynamic nature of AKs makes them excellent targets to study protein flexibility and temperature adaptation since flexibility is directly related to activity and stability. The monomeric state of the *Bacillus* AKs is also desirable because they lack the quaternary structure that can complicate kinetic and structural analysis. A wealth of information regarding their biochemistry has facilitated this study.

Before analyzing target proteins for temperature adaptation, they should be examined for their intrinsic temperature-related properties. Proteins from temperature extremophiles most likely have the same temperature preferences as their source organisms, but this is not always guaranteed. In fact, cytosolic solutes stabilizing proteins at high temperatures have been found in various thermophilic organisms (43, 44). DSC and activity assays for the three AKs confirmed their intrinsic adaptation to different temperatures. DSC results of AK·Ap5A complexes showed that the differences between AKs were also maintained between AK·Ap5A complexes. This result suggests that the principles underlying the thermal stability differences between AKs are also present in the case of inhibitor-bound complexes and validates drawing conclusions about AKs based on AK·Ap5A structures. In the activity assays, the psychrophilic AKglo showed maximal activity at 35 °C that is higher than the optimal growth temperature of its source organism. This incomplete adaptation to cold temperature has been found in almost all characterized enzymes from psychrophilic organisms and has even been proposed as a basic feature of psy-

TABLE V
Critical ion pairs in Bacillus AKs

Structures compared		Structures compared		Structures compared	
AKste	AKsub	AKste	AKglo	AKsub	AKglo
Lys-19–Glu-202 Arg-116–Glu-198 Arg-131–Glu-156 Lys-180–Asp-114	None	Lys-19–Glu-202 Arg-116–Glu-198 Arg-131–Glu-156 Lys-180–Asp-114	Lys-23–Asp-209 Lys-152–Asp18	None	None

chrophilic enzymes (17). The possibility of cytosolic factors that may increase the activity of psychrophilic enzymes at low temperatures similar to the stabilizing solutes for thermophilic enzymes has been proposed (45), but the evidence of such factors is slight.

For adaptation to high temperatures, AKste seems to use electrostatic interactions of ion pairs. Even though the differences in the number of ion pairs may not appear to be dramatic, the difference in the stability between thermophilic and mesophilic proteins sometimes requires only a single extra ion pair (10, 46). Moreover, AKste has three to four more critical ion pairs that are thought to be more important (Fig. 5). This suggests that the electrostatic interactions of the ion pairs in AKste may contribute to its increased stability at high temperatures, although mutational studies for the ion pairs are needed to give more conclusive answers. It is not surprising that AKglo and AKsub essentially have the same number of ion pairs because electrostatic interactions conferred by ion pairs contribute to protein stabilization mostly at high temperatures due to the markedly reduced desolvation penalty for the formation of ion pairs at high temperatures (41). A strong correlation is also found between thermal stability and apolar buried surface area of the AKs. The more stable an AK, the more apolar buried surface area it has. The difference between AKste and AKsub is 251 Å^2 and is approximately equivalent to 2.1–5.6 kcal/mol of hydrophobic interactions. The gap between AKsub and AKglo is even larger. It is 483 Å^2 and could be equivalent to 4.0–10.8 kcal/mol. These are probably sufficient amounts of energy to explain the different thermal stabilities of the trio considering that the free energy of stabilization of globular proteins is typically between 5 and 15 kcal/mol at 25 °C, and the differences in the free energy between thermophilic, mesophilic, and psychrophilic proteins are usually of the same order of magnitude (3, 17, 46). The *Bacillus* AK structures appear to adapt themselves to different environmental temperatures through changes in non-covalent intramolecular interactions, which are electrostatic and hydrophobic interactions for heat adaptation of AKste and hydrophobic interactions for cold adaptation of AKglo. It is interesting to note that thermophilic AKs from the genus *Methanococcus* exhibited a similar molecular mechanism for their heat adaptation (11).

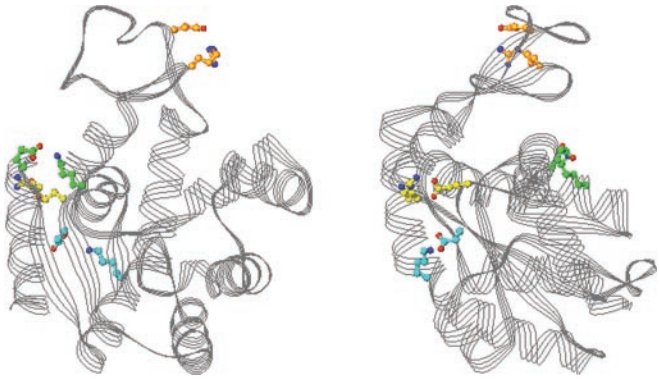

FIG. 5. **Critical ion pairs in AKste.** *Left*, AKste with its critical ion pairs is seen in the same orientation as in Fig. 3*C*. *Right*, the same structure rotated 90°. The critical ion pairs spread over the AKste structure and bridge distant regions of a polypeptide. Side chains of the critical ion pairs are shown as *ball and stick* models with the AKste backbone drawn as *thin gray lines*. Nitrogen and oxygen atoms are shown in *blue* and *red*, respectively. The ion pairs are shown in different colors; *green* for Lys-19—Glu-202, *yellow* for Arg-116—Glu-198, *orange* for Arg-131—Glu-156, and *cyan* for Lys-180—Asp-114.

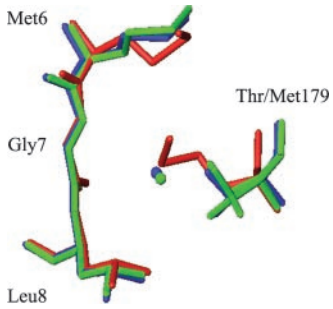

FIG. 6. **Effect of residue 179 substitution on hydrophobic interactions in *Bacillus* AKs.** In AKste the side chain of Met-179 fits into a hydrophobic pocket made by Met-6, Gly-7, and Leu-8, resulting in the burial of hydrophobic surface. Residues 6–8 and 179 of AKglo, AKsub, and AKste are shown as *blue*, *green*, and *red stick models*, respectively. Multiple conformers of Thr-179 of AKsub are all shown. Water molecules in AKglo and AKsub are represented at the center as *blue* and *green spheres*, respectively.

Because of highly homologous nature of the *Bacillus* AKs, it was possible to find specific residue substitutions that may contribute to temperature adaptation by altering hydrophobic interactions. Residue 179 is one of them. The psychrophilic AKglo and mesophilic AKsub have a Thr residue in this position, whereas the thermophilic AKste has a Met. In AKste, this Met residue is involved in hydrophobic interactions with residues in a distant region of the polypeptide. The Met-179 side chain fits into a hydrophobic pocket made by Met-6, Gly-7, and Leu-8 (Fig. 6). Even though Met-6, Gly-7, and Leu-8 are conserved in AKglo and AKsub, Thr-179 cannot make such a contact, and the hydrophobic surface is substantially more solvent-exposed than in AKste (Table VI). In the models of AKglo and AKsub, a water molecule occupies this pocket. Another example of residue substitutions modifying hydrophobic interactions occurs in AKglo. The substitution of Thr-26 in AKglo for Ile-26 in AKste and AKsub results in a drastic change in solvent accessibility of the adjacent Val-21, which is conserved through all three AKs. The exposed surface area of the Val residue is 23 and 27 Å^2 in AKste and AKsub, respectively, but increases to 42 Å^2 in AKglo. Because Val-21 participates in the hydrophobic cores of the AK structures, this substitution may affect the overall stability/flexibility and cold adaptation of the psychrophilic AKglo.

Regulating stability by modifying the intramolecular interactions is thought to be a result of efforts to maintain proper flexibility to perform a catalytic reaction at different temperatures. It is expected that backbone dynamics, at least in some area of the AKs, would correlate with their temperature/activity profiles. Even though it is impossible to completely describe the motion of proteins in crystals, crystallographic data may give insight into protein dynamics. Crystallographic B-factors may be related to intrinsic flexibility of proteins, although they depend on many other sources of disorders. One hypothesis is

TABLE VI
Effect of residue 179 substitution on solvent accessibility

	Amino acid	Exposed surface area	Amino acid	Exposed surface area	Amino acid	Exposed surface area	Amino acid	Exposed surface area
		Å^2		Å^2		Å^2		Å^2
AKglo	Met-6	10	Gly-7	19	Leu-8	27	Thr-179	22
AKsub	Met-6	13	Gly-7	22	Leu-8	38	Thr-179	48
AKste	Met-6	4	Gly-7	4	Leu-8	7	Met-179	3

that AKglo is more flexible and harder to confine in a small space than AKste or AKsub and, therefore, requires a different crystal form providing more space per molecule for conformational entropy. There is, in fact, a correlation between the B-factors and temperature optima of the AKs. The average B-factors of main chain atoms for AKglo, AKsub, and AKste are 49.5, 27.7, and 10.9 Å^2, respectively. The same correlation is found with B-factors from Wilson plots. Considering the same crystallization temperature (20 °C) for all three AKs, this suggests that the flexibilities of the AKs may also be correlated with their optimal operating temperatures. The flexible nature of AKglo is also found in other data. AKglo has the fewest contacting residues with neighboring molecules in the crystal lattice and the largest specific volume and solvent content among the AKs. These properties of AKglo result from sparse crystal packing, which may be caused by its high intrinsic mobility, although other factors could produce this trend as well.

Other than becoming too rigid to function, another challenge faced by proteins at lower than optimal temperatures is that proteins lose their active configuration at lower temperatures, so-called "cold denaturation." The role of entropy and dynamics in cold denaturation is likely as follows (47). Water, as it cools, takes on a more ordered structure. The penalty for having a hydrophobe in the solvent is diminished, since the water is already ordered, and the hydrophobic effect is entropy driven. The contrast between the interior and exterior of the protein is, therefore, compromised and the protein loses native configuration (48). It is interesting to note that the psychrophilic AKglo has been observed to have about 200 Å^2 more apolar-exposed surface area than the mesophilic AKsub and thermophilic AKste, suggesting that protection against cold denaturation might include a design selection that has more "strategically" pre-exposed hydrophobic surface so as not to risk losing native configurations due to this effect. An increase of exposed apolar surface area in a psychrophilic protein relative to its mesophilic or thermophilic counterpart is also observed in other examples such as xylanase from Antarctic bacteria (15) and trypsin from Atlantic salmon (49).

In conclusion, a set of structures of the three highly homologous, dynamic proteins with different temperature-activity profiles have been solved. The analysis of the structures suggests that the maintenance of proper flexibility is critical for proteins to function at their environmental temperatures and is achieved by the modification of intramolecular interactions in the process of temperature adaptation. It is obvious that dynamics and mutational studies are required to explore more integrated and detailed mechanisms for cold and heat adaptation. These studies are currently under way.

Acknowledgments—We are grateful to Dr. A.-M. Gilles and Dr. O. Bârzu for providing a partial amino acid sequence of AKglo. We thank the staff of the BioCARS beamline at the Advanced Photon Source for support with data collection, Dr. D. R. McCaslin for assistance with DSC experiments at the University of Wisconsin-Madison Biophysics Instrumentation Facility, and J. G. McCoy for comments on the manuscript.

REFERENCES

1. Rothschild, L. J., and Mancinelli, R. L. (2001) *Nature* **409,** 1092–1101
2. Deming, J. W. (2002) *Curr. Opin. Microbiol.* **5,** 301–309
3. Jaenicke, R., and Böhm, G. (1998) *Curr. Opin. Struct. Biol.* **8,** 738–748
4. Demirjian, D. C., Moris-Varas, F., and Cassidy, C. S. (2001) *Curr. Opin. Chem. Biol.* **5,** 144–151
5. Bruins, M. E., Janssen, A. E., and Boom, R. M. (2001) *Appl. Biochem. Biotechnol.* **90,** 155–186
6. D'Amico, S., Marx, J. C., Gerday, C., and Feller, G. (2003) *J. Biol. Chem.* **278,** 7891–7896
7. Lonhienne, T., Gerday, C., and Feller, G. (2000) *Biochim. Biophys. Acta* **1543,** 1–10
8. Szilágy, A., and Závodszky, P. (2000) *Structure* **8,** 493–504
9. Tanner, J. J., Hecht, R. M., and Krause, K. L. (1996) *Biochemistry* **35,** 2597–2609
10. Perl, D., Mueller, U., Heinemann, U., and Schmid, F. X. (2000) *Nat. Struct. Biol.* **7,** 380–383
11. Criswell, A. R., Bae, E., Stec, B., Konisky, J., and Phillips, G. N., Jr. (2003) *J. Mol. Biol.* **330,** 1087–1099
12. Russell, N. J. (2000) *Extremophiles* **4,** 83–90
13. Aghajari, N., Feller, G., Gerday, C., and Haser, R. (1998) *Structure* **6,** 1503–1516
14. Kim, S. Y., Hwang, K. Y., Kim, S. H., Sung, H. C., Han, Y. S., and Cho, Y. (1999) *J. Biol. Chem.* **274,** 11761–11767
15. Van Petegem, F., Collins, T., Meuwis, M. A., Gerday, C., Feller, G., and Van Beeumen, J. (2003) *J. Biol. Chem.* **278,** 7531–7539
16. Gianese, G., Bossa, F., and Pascarella, S. (2002) *Proteins* **47,** 236–249
17. D'Amico, S., Claverie, P., Collins, T., Georlette, D., Gratia, E., Hoyoux, A., Meuwis, M. A., Feller, G., and Gerday, C. (2002) *Philos. Trans. R. Soc. Lond. B. Biol. Sci.* **357,** 917–925
18. Fields, P. A. (2001) *Comp. Biochem. Physiol. A. Mol. Integr. Physiol.* **129,** 417–431
19. Sheridan, P. P., Panasik, N., Coombs, J. M., and Brenchley, J. E. (2000) *Biochim. Biophys. Acta* **1543,** 417–433
20. Gilles, A. M., Glaser, P., Perrier, V., Meier, A., Longin, R., Sebald, M., Maignan, L., Pistotnik, E., and Barzu, O. (1994) *J. Bacteriol.* **176,** 520–523
21. Perrier, V., Surewicz, W. K., Glaser, P., Martineau, L., Craescu, C. T., Fabian, H., Mantsch, H. H., Barzu, O., and Gilles, A. M. (1994) *Biochemistry* **33,** 9960–9967
22. Glaser, P., Presecan, E., Delepierre, M., Surewicz, W. K., Mantsch, H. H., Barzu, O., and Gilles, A. M. (1992) *Biochemistry* **31,** 3038–3043
23. Claus, D., and Berkeley, R. C. W. (1986) in *Bergey's Manual of Systematic Bacteriology* (Sneath, P. H. A., ed) Vol. 2, pp. 1105–1139, Williams & Wilkins, Baltimore
24. Noda, L. (1973) in *The Enzymes* (Boyer, P. D., ed) Vol. 8, 3rd Ed., pp. 279–305, Academic Press, Inc., New York
25. Vonrhein, C., Schlauderer, G., and Schulz, G. E. (1995) *Structure* **3,** 483–490
26. Gerstein, M., Schulz, G., and Chothia, C. (1993) *J. Mol. Biol.* **229,** 494–501
27. Schulz, G. E. (1987) *Cold Spring Harbor Symp. Quant. Biol.* **52,** 429–439
28. Müller, C. W., and Schulz, G. E. (1992) *J. Mol. Biol.* **224,** 159–177
29. Berry, M. B., and Phillips, G. N., Jr. (1998) *Proteins Struct. Funct. Genet.* **32,** 275–288
30. Müller, C. W., Schlauderer, G. J., Reinstein, J., and Schulz, G. E. (1996) *Structure* **4,** 147–156
31. Rayment, I. (2002) *Structure* (*Camb*) **10,** 147–151
32. Otwinowski, Z., and Minor, W. (1997) *Methods Enzymol.* **276,** 307–326
33. Jamrog, D. C., Zhang, Y., and Phillips, G. N., Jr. (2003) *Acta Crystallogr. Sect. D Biol. Crystallogr.* **59,** 304–314
34. Brunger, A. T., Adams, P. D., Clore, G. M., Delano, W. L., Gros, P., Grosse-Kunstleve, R. W., Jiang, J. S., Kuszewski, J., Nilges, N., Pannu, N. S., Read, R. J., Rice, L. M., Simonson, T., and Warren, G. L. (1998) *Acta Crystallogr. Sect. D Biol. Crystallogr.* **54,** 905–921
35. McRee, D. E. (1999) *J. Struct. Biol.* **125,** 156–165
36. Laskowski, R. A., MacArthur, M. W., Moss, D. S., and Thornton, J. M. (1993) *J. Appl. Crystallogr.* **26,** 283–291
37. Bruns, C. M., Hubatsch, I., Ridderström, M., Mannervik, B., and Tainer, J. A. (1999) *J. Mol. Biol.* **288,** 427–439
38. Vriend, G. (1990) *J. Mol. Graph.* **8,** 52–56
39. Carson, M. (1997) *Methods Enzymol.* **277,** 493–505
40. Alberts, I. L., Nadassy, K., and Wodak, S. J. (1998) *Protein Sci.* **7,** 1700–1716
41. Elcock, A. H. (1998) *J. Mol. Biol.* **284,** 489–502
42. Shi, Z., Krantz, B. A., Kallenbach, N., and Sosnick, T. R. (2002) *Biochemistry* **41,** 2120–2129
43. Hensel, R., and König, H. (1988) *FEMS Microbiol. Lett.* **49,** 75–79
44. Martins, L. O., Carreto, L. S., Da Costa, M. S., and Santos, H. (1996) *J. Bacteriol.* **178,** 5644–5651
45. Thomas, T., and Cavicchioli, R. (2000) *J. Bacteriol.* **182,** 1328–1332
46. Vieille, C., and Zeikus, G. J. (2001) *Microbiol. Mol. Biol. Rev.* **65,** 1–43
47. Privalov, P. L. (1990) *Crit. Rev. Biochem. Mol. Biol.* **25,** 281–305
48. Tsai, C. J., Maizel, J. V., Jr., and Nussinov, R. (2002) *Crit. Rev. Biochem. Mol. Biol.* **37,** 55–69
49. Smalas, A. O., Heimstad, E. S., Hordvik, A., Willassen, N. P., and Male, R. (1994) *Proteins* **20,** 149–166
50. Thompson, J. D., Higgins, D. G., and Gibson, T. J. (1994) *Nucleic Acids Res.* **22,** 4673–4680